

Supporting Information for

Nanoengineered mitochondria enable ocular mitochondrial disease therapy *via* the replacement of dysfunctional mitochondria

Yi Wang^{a,†}, Nahui Liu^{a,†}, Lifan Hu^{a,†}, Jingsong Yang^a, Mengmeng Han^a, Tianjiao Zhou^a, Lei Xing^{a,*}, Hulin Jiang^{a,b,*}

^a*State Key Laboratory of Natural Medicines, China Pharmaceutical University, Nanjing, 210009, China*

^b*College of Pharmacy, Yanbian University, Yanji, 133002, China*

*Corresponding authors. Tel./fax: +86 025 83271027 (Hulin Jiang, Lei Xing). E-mail addresses: jianghulin3@163.com (Hulin Jiang), xinglei6xl@163.com (Lei Xing).

[†]These authors made equal contributions to this work.

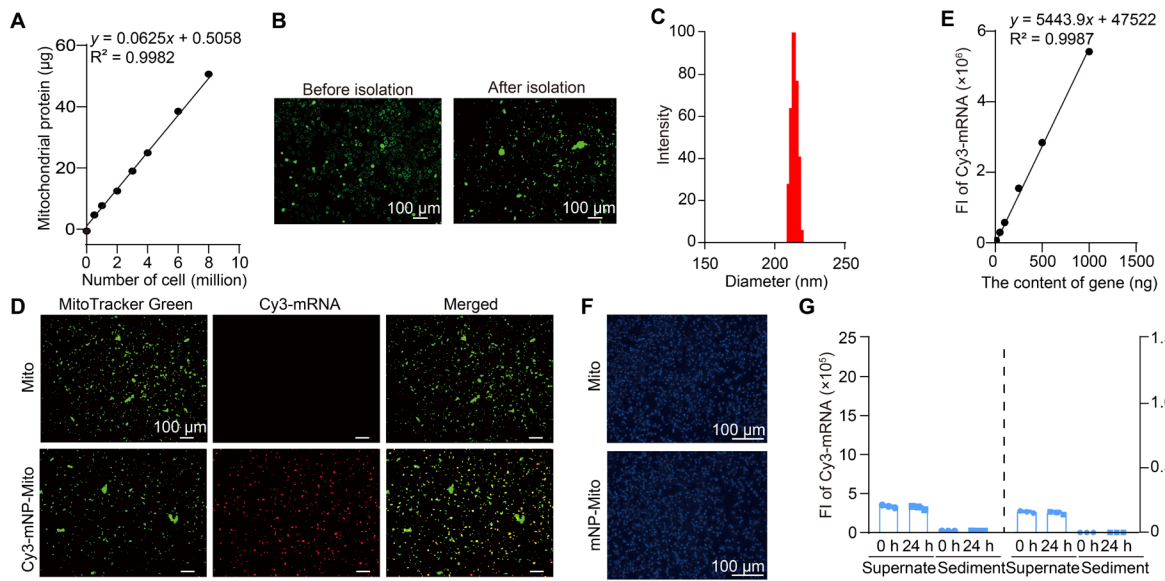


Figure S1 The characteristics of mNP-Mito. (A) The standard curve of mitochondrial proteins and the number of donor cells; (B) Before isolation from donor cells and after isolation in a culture dish, the mitochondrial mass was detected by MitoTracker Green probe; (C) The nanoparticle size of mNP; (D) The binding of Cy3-mNP to extracted mitochondria checked by the colocalization of green-labeled mitochondria and red-labeled mRNA; (E) The relationship between fluorescence intensity (FI) of Cy3-mRNA and the contents of mRNA; (F) The mitochondrial activity before and after binding with mNP detected by Janus green-B dye; (G) FI of Cy3-mRNA was used to investigate the stability of mNP-Mito at different times.

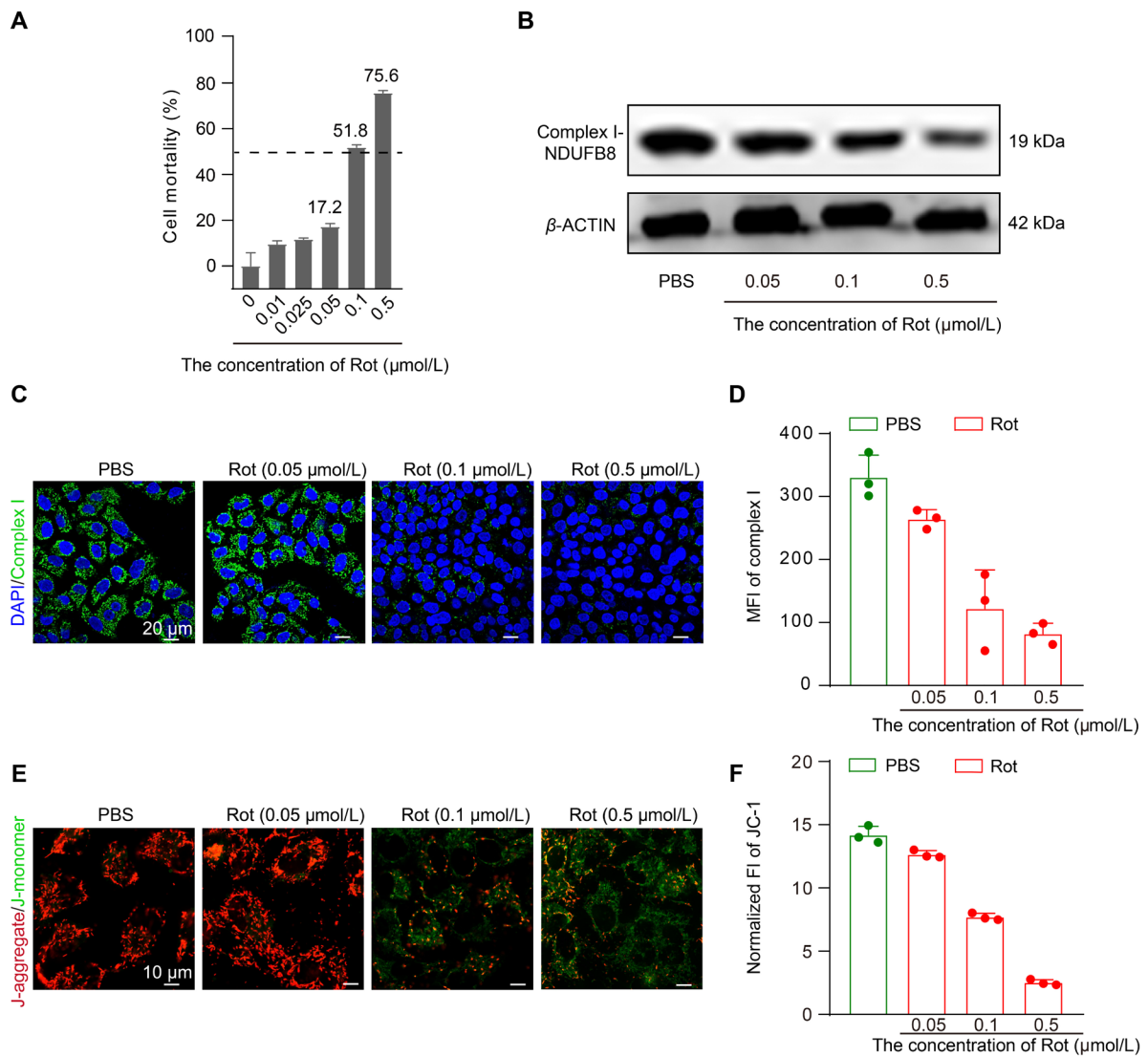


Figure S2 Impairment of mitochondrial complex I tightly correlates with Rot concentrations in the Rot-induced cell model. (A) The relationship between Rot concentration and cell mortality; (B) The expression of mitochondrial protein NDUFB8 was evaluated under different concentrations of Rot *in vitro*; (C, D) Decreasing complex I contents detected by CLSM (C) and flow cytometry of extracted mitochondria (D); (E, F) The changes in MMP detected by CLSM (E) and multifunctional microplate reader (F), normalized FI = FI/cellular whole-protein contents. In (A), (D), and (F), data are mean \pm SD ($n = 3$).

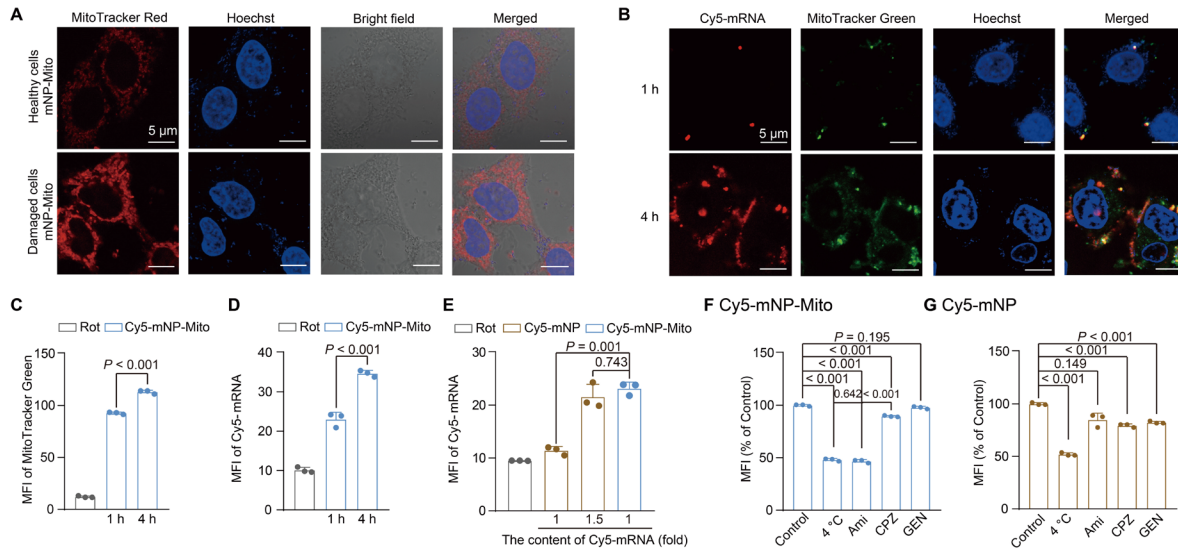


Figure S3 The cellular uptake of mNP-Mito. (A) The cellular uptake of exogenous mitochondria in normal HeLa cells and Rot-damaged cells (24 h); (B–D) The cellular uptake of MitoTracker Green-labeled Cy5-mNP-Mito after different treatment times detected by CLSM (B) and flow cytometer (C, D); (E) The cellular uptake of Cy5-mNP-Mito after different treatments at 4 h detected by flow cytometer; (F, G) The cellular endocytosis pathway studies of Cy5-mNP-Mito (F) and Cy5-mNP (G). Data are shown as mean \pm SD ($n = 3$ in C–G). Statistical significance was analyzed by one-way ANOVA with the Tukey’s honest significant difference (HSD) post hoc test (C, D, F) and Games-Howell test (E, G).

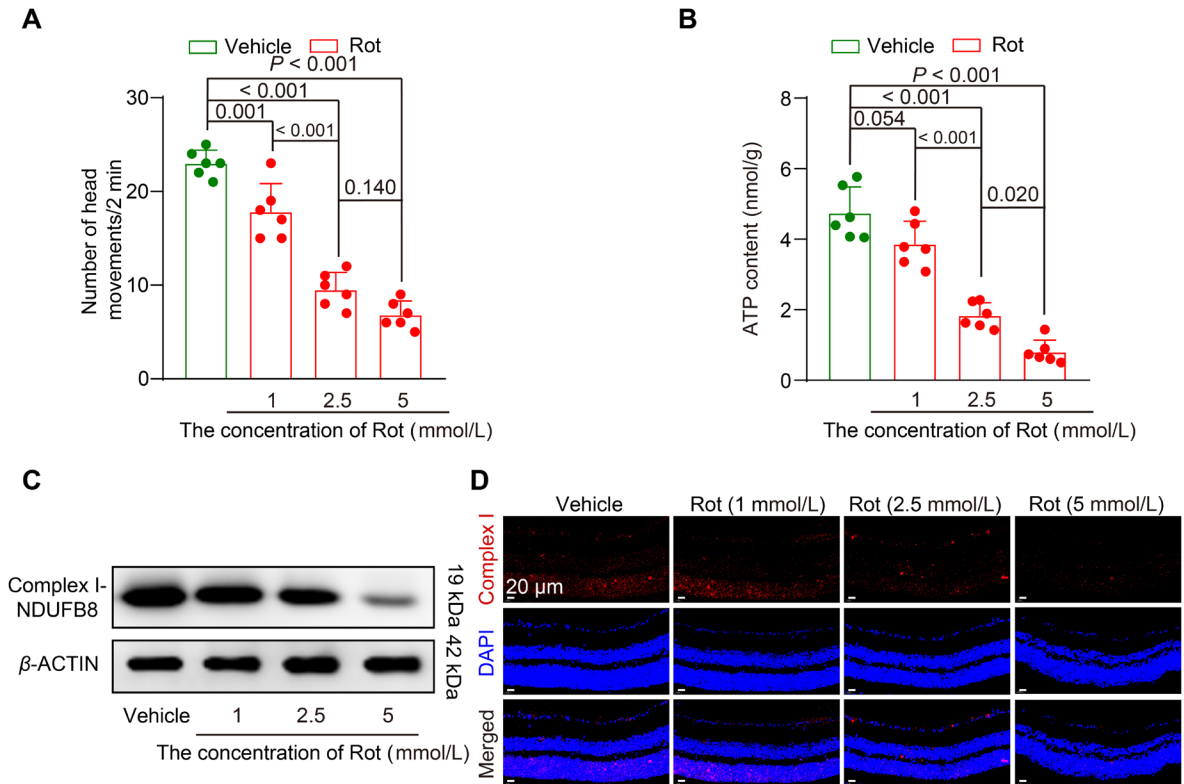


Figure S4 Impairment of mitochondrial complex I tightly correlates with disorder severity in the Rot-induced experimental LHON-like mouse model. (A) The optomotor test and counting the number of head movements following different Rot concentrations; (B) ATP contents in retina after treatment with different concentrations of Rot; (C) The expression of mitochondrial protein NDUFB8 located in mitochondrial complex I after Rot treatment; (D) The contents of complex I detected by immunofluorescence staining after Rot treatment. Data are shown as mean \pm SD ($n = 6$ in A, B). Statistical significance was analyzed by one-way ANOVA with the Tukey's honest significant difference (HSD) post hoc test (A, B).

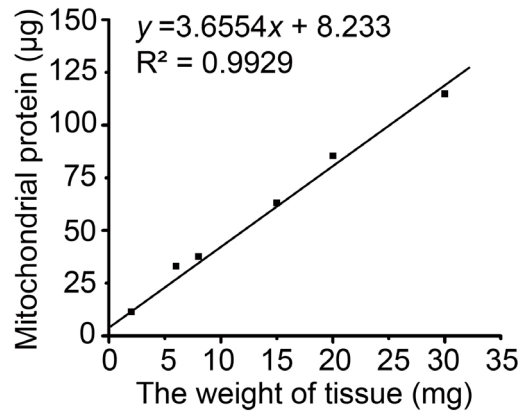


Figure S5 The standard curve between the weight of Balb/c mouse heart tissues and the contents of mitochondrial proteins.

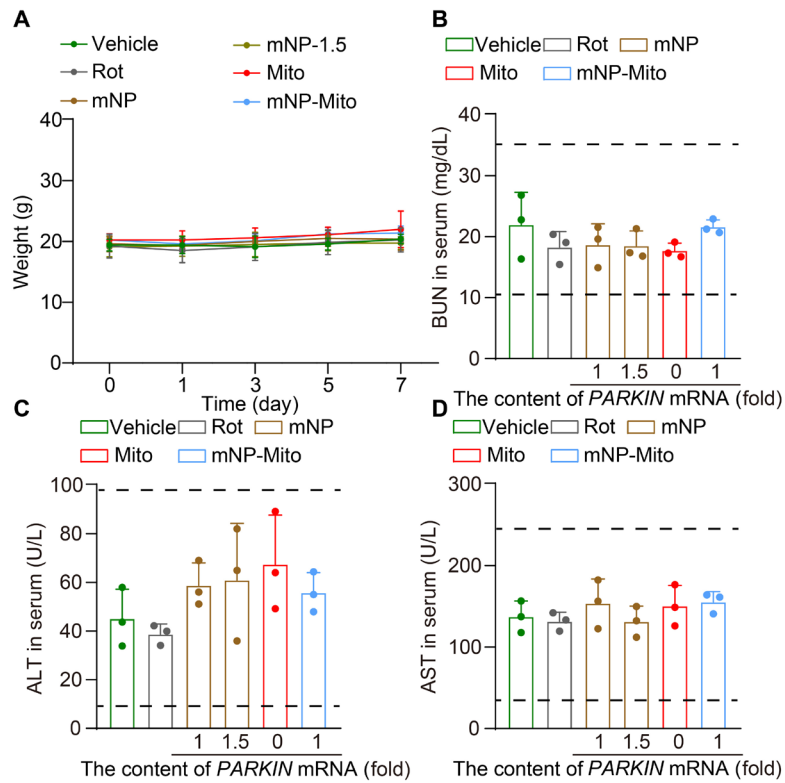


Figure S6 The safety of mNP-Mito in Rot-induced mice model. (A) The weight change in different formulation treatments; (B–D) The detection of blood urea nitrogen (BUN, B), alanine transaminase (ALT, C), and aspartate aminotransferase (AST, D) in serum after Day 7 of treatments, error bars: mean \pm SD ($n = 7$ per group in A, $n = 3$ mice per group in B–D). The dashed area represents the normal range of the indicator.

Table S1 The organ indexes of the normal Balb/c mice in PBS, Low-dose (1-fold mNP-Mito), Mid-dose (2-fold mNP-Mito) and High-dose (4-fold mNP-Mito) groups after Day 14 treatments (intravitreal administration, organ index = organ/body weight \times 100), $n = 6$ in the PBS, Low-dose and Mid-does groups, $n = 5$ in the High-dose group. Statistical significance was measured using one-way ANOVA with the Scheffe or Games-Howell test. Each group was compared with the PBS group, with a $P > 0.05$. Except for PBS (liver) *versus* High-dose (liver) group, $P = 0.022$; and PBS (liver) *versus* Mid-dose (liver) group, $P = 0.045$. Error bars: mean \pm SD.

Organ	PBS	Low-dose group	Mid-dose group	High-dose group
Heart	0.49 \pm 0.06	0.48 \pm 0.02	0.48 \pm 0.07	0.49 \pm 0.04
Liver	4.33 \pm 4.25	4.84 \pm 0.21	4.88 \pm 0.23	4.97 \pm 0.44
Spleen	0.51 \pm 0.08	0.59 \pm 0.06	0.56 \pm 0.04	0.57 \pm 0.12
Lung	0.70 \pm 0.07	0.79 \pm 0.04	1.11 \pm 0.90	0.74 \pm 0.08
Kidney	1.44 \pm 0.13	1.58 \pm 0.06	1.58 \pm 0.06	1.39 \pm 0.14

Table S2 The hematological parameters of the mice in various groups after different treatments in the LHON mice model. Error bars: mean \pm SD ($n = 3$ mice per group).

–	Vehicle	Rot	mNP	mNP-1.5	Mito	mNP-Mito	Reference
WBC	5.50 \pm 1.61	6.87 \pm 5.05	4.57 \pm 1.63	2.23 \pm 1.60	3.33 \pm 0.72	5.30 \pm 1.57	0.80–6.80
Lymph	3.57 \pm 0.83	3.50 \pm 2.17	3.30 \pm 1.39	1.63 \pm 1.14	2.50 \pm 0.66	3.90 \pm 1.30	0.70–5.70
Gran	1.30 \pm 0.17	1.30 \pm 0.44	1.03 \pm 0.31	0.53 \pm 0.42	0.73 \pm 0.23	1.23 \pm 0.59	0.10–1.80
Lymph%	65.33 \pm 3.11	62.17 \pm 9.51	70.40 \pm 7.57	73.07 \pm 1.07	75.40 \pm 6.56	72.93 \pm 9.78	55.80–90.60
Mon%	5.13 \pm 0.40	6.47 \pm 3.32	6.10 \pm 3.77	3.67 \pm 0.32	3.47 \pm 1.01	3.93 \pm 1.72	1.80–6.00
Gran%	29.20 \pm 3.33	31.37 \pm 10.37	23.50 \pm 3.80	23.27 \pm 1.01	21.13 \pm 5.61	23.13 \pm 8.17	8.60–38.90
HGB	141.67 \pm 10.01	146.33 \pm 24.17	148.67 \pm 4.04	137.33 \pm 6.35	140.67 \pm 16.04	134.00 \pm 3.00	110.00–143.00
HCT	39.90 \pm 2.69	34.97 \pm 2.06	39.93 \pm 4.53	37.23 \pm 4.46	35.30 \pm 3.05	35.73 \pm 2.93	34.60–44.60
MCHC	319.33 \pm 17.16	347.00 \pm 22.61	333.33 \pm 30.50	337.33 \pm 21.08	332.67 \pm 19.66	313.00 \pm 12.49	302.00–353.00

WBC: white blood cells; Lymph: lymphocytes; Gran: granulocytes; Lymph%: lymphocyte percentage; Mon%: monocyte percentage; Gran%: granulocyte percentage; HGB: hemoglobin; HCT: hematocrit; MCHC: mean corpuscular hemoglobin concentration.